

## Synchrotron-radiation study of Fe 3d states in $\text{Cd}_{1-x}\text{Fe}_x\text{Se}$ ( $0 \leq x \leq 0.4$ )

M. Taniguchi

*Department of Materials Science, Faculty of Science, Hiroshima University, Higashisenda-machi, Naka-ku, Hiroshima 730, Japan*

Y. Ueda

*Department of Physics, Tokuyama National College of Technology, Kume, Tokuyama 745, Japan*

I. Morisada, Y. Murashita, and T. Ohta

*Department of Materials Science, Faculty of Science, Hiroshima University, Higashisenda-machi, Naka-ku, Hiroshima 730, Japan*

I. Souma and Y. Oka

*Research Institute for Scientific Measurements, Tohoku University, Katahira, Sendai 980, Japan*

(Received 16 August 1989)

The electronic structure of  $\text{Cd}_{1-x}\text{Fe}_x\text{Se}$  ( $0 \leq x \leq 0.4$ ) has been investigated by synchrotron-radiation photoemission in the photon energy range from 47 to 62 eV. Valence-band photoemission spectra of  $\text{Cd}_{0.6}\text{Fe}_{0.4}\text{Se}$  exhibit Fe-derived narrow peaks at 0.5 and 3.7 eV below the valence-band maximum. These structures are assigned to emission from the Fe 3d $\downarrow$  and 3d $\uparrow$  states with  $e_g$  symmetry, respectively. The  $t_{2g}$  components hybridize appreciably with the Se 4p states and contribute throughout the top 6 eV of the valence bands. The results are qualitatively interpreted in terms of a molecular-orbital level scheme.

### I. INTRODUCTION

$\text{Cd}_{1-x}\text{Fe}_x\text{Se}$  mixed crystals are substitutional solid solutions in which Fe atoms replace Cd atoms in the wurtzite structure of CdSe. Magnetic and magneto-optical properties of  $\text{Cd}_{1-x}\text{Fe}_x\text{Se}$  crystals differ significantly from those of the better known Mn-substituted II-VI compound semiconductors such as  $\text{Cd}_{1-x}\text{Mn}_x\text{Te}$ ,  $\text{Cd}_{1-x}\text{Mn}_x\text{Se}$ , and  $\text{Cd}_{1-x}\text{Mn}_x\text{S}$ .<sup>1-3</sup> Information about energy positions of 3d levels of dilute magnetic ions and hybridization of the 3d states with the sp valence-band states plays an important role for understanding the physical nature of these materials.

Baranowski and Langer<sup>4</sup> placed the  $\text{Fe}^{2+}$  (3d) level in doped CdSe with an Fe concentration of  $1.5 \times 10^{19} \text{ cm}^{-3}$  at  $0.63 \pm 0.02$  eV above the top of the valence bands from their optical-absorption measurements. For an Fe-doped CdSe sample with a concentration up to 15 at. % ( $5 \times 10^{21} \text{ cm}^{-3}$ ), Mycielski *et al.*<sup>5</sup> reported the  $\text{Fe}^{2+}$  level at  $0.58 \pm 0.03$  eV above the valence-band maximum from the analysis of the optical-absorption spectra. Very recently, Kisiel *et al.*<sup>6</sup> have proposed a one-electron schematic diagram of the splitting and hybridization of the  $\text{Fe}^{2+}$  states in  $\text{Cd}_{1-x}\text{Fe}_x\text{Se}$  based on their optical-reflectivity data in the energy range from 4 to 10 eV. According to the diagram, the density of states (DOS) of valence bands for  $\text{Cd}_{1-x}\text{Fe}_x\text{Se}$  consists of three constituents labeled A, B, and C. The structure C located at the top region of valence bands is assumed to originate from hybridized Fe 3d states. In addition, the structure A placed below the Se 4p valence bands (B) is considered to be due to the nonhybridized Fe 3d orbitals. Crucial information about the Fe 3d levels, their width, and their

degree of hybridization with the Se 4p bands is, however, still lacking so far.

In this paper, we report an unambiguous identification of the Fe 3d states in  $\text{Cd}_{1-x}\text{Fe}_x\text{Se}$  ( $0 \leq x \leq 0.4$ ) by photoemission using synchrotron radiation. For  $x = 0.4$ , Fe 3d (down-spin,  $\downarrow$ ) and 3d (up-spin  $\uparrow$ ) bands with  $e_g$  symmetry are observed as narrow peak structures at 0.5 and 3.7 eV below the valence-band maximum, respectively, whereas the remainder of the 3d electrons with  $t_{2g}$  symmetry are found to contribute to the top 6 eV of valence bands.

### II. EXPERIMENT

The present photoemission experiments were performed by using synchrotron radiation from SOR-RING (an electron storage ring operated at 380 MeV) at the Institute for Solid State Physics of The University of Tokyo. A combination of a modified Rowland-type monochromator and a double-stage cylindrical-mirror analyzer was used to measure the angle-integrated photoemission spectra. Binding energy with respect to the top of valence bands was determined by extrapolating the steep leading edge of the highest valence-band peak to the baseline. The samples used were undoped single crystals grown by a modified Bridgman method with Fe concentrations of 0, 0.2, 0.3, and 0.4, respectively. Surfaces for the photoemission measurements were prepared by cleavage under ultrahigh vacuum ( $< 3 \times 10^{-10}$  Torr) in the preparation chamber. Then, the sample was transferred into the analyzer chamber with a working pressure of  $7 \times 10^{-11}$  Torr.

### III. RESULTS AND DISCUSSIONS

Figure 1 shows valence-band photoemission spectra of  $\text{Cd}_{1-x}\text{Fe}_x\text{Se}$  for Fe concentrations of 0, 0.2, and 0.4 measured at an excitation photon energy ( $\hbar\omega$ ) of 47 eV. The valence-band spectrum of pure CdSe has been discussed in detail by Ley *et al.*<sup>7</sup> We recall here that the two prominent peaks at 1.2- and 4.0-eV binding energies ( $p$  valence bands) reflect maxima in the DOS which are primarily derived from Se  $4p$  states with an increasing contribution from the Cd  $5s$  state toward deeper binding energy. With increasing Fe concentration from 0 to 0.2, we find a new weak structure above the valence-band maximum of CdSe. For  $\text{Cd}_{0.8}\text{Fe}_{0.2}\text{Se}$ , we define the top of the valence bands by extrapolating the leading edge of the weak Fe-induced peak to the baseline. Thus, the binding energy of this peak is estimated to be 0.5 eV with respect to the new valence-band maximum. At  $x=0.4$ , one can recognize an increasing Fe component between two prominent  $p$  valence bands as well as the small peak at 0.5 eV.

In addition to the concentration-dependence of valence-band spectra, the identification of the Fe  $3d$ -derived states is considerably facilitated by the use of tunable synchrotron radiation. We can evaluate a measure of the Fe-derived partial DOS and investigate the degree of hybridization in  $\text{Cd}_{1-x}\text{Fe}_x\text{Se}$  in detail from resonant photoemission measurements.<sup>8-10</sup> The resonance takes place in a particular energy region as a result of an interference between the direct excitation process of the Fe  $3d$  electrons ( $3p^63d^6 \rightarrow 3p^63d^5 + \epsilon l$ ) and the discrete Fe  $3p \rightarrow 3d$  excitation process followed by a super Coster-Kronig decay ( $3p^63d^6 \rightarrow 3p^53d^7, 3p^53d^7 \rightarrow 3p^63d^5 + \epsilon l$ ). Since only the Fe  $3d$  states are resonantly enhanced for  $\hbar\omega$  near the Fe  $3p \rightarrow 3d$  excitation, we can estimate their contribution to the valence-band DOS by comparing spectra taken on and off resonance. The

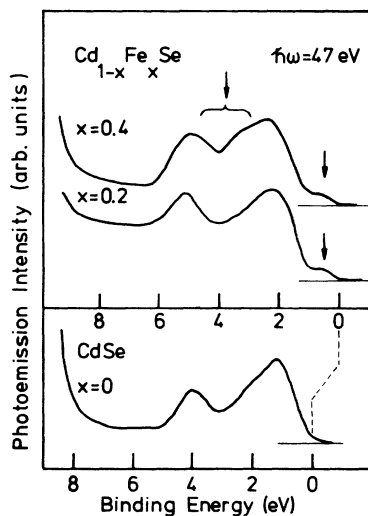


FIG. 1. Valence-band photoemission spectra of  $\text{Cd}_{1-x}\text{Fe}_x\text{Se}$  for different Fe concentrations measured at  $\hbar\omega=47$  eV. Fe-derived features are marked by vertical arrows. Binding energy is defined relative to the valence-band maximum.

cross section of the remaining valence states (Se  $4p$  and Cd  $5s, 5p$ ) do not vary appreciably over the small energy region of the resonance.

Figure 2 shows a series of valence-band spectra of  $\text{Cd}_{0.6}\text{Fe}_{0.4}\text{Se}$  for  $\hbar\omega$  in the Fe  $3p \rightarrow 3d$  excitation region. The intensities have been normalized to the monochromator output. One notices four structures at 0.5, 2.3, 3.7, and 5.0 eV binding energies below the valence-band maximum as shown by vertical arrows for the spectrum taken at  $\hbar\omega=56$  eV. Among these structures, the peak at 3.7 eV exhibits a prominent resonance. With increasing  $\hbar\omega$  from 47 to 62 eV, the intensity of this peak first decreases gradually until its minimum at  $\hbar\omega=52$  eV and then reaches its maximum at  $\hbar\omega=56$  eV. The remainder of the valence bands in the energy range from 0 to 6 eV are also resonantly enhanced to a lesser extent.

In order to see the shape of the resonance and its amplitude, we plot the photoemission intensities of selected valence bands as a function of  $\hbar\omega$  in Fig. 3, where each valence band is specified by the binding energy ( $E_i$ ) with respect to the valence-band maximum. One notices that the spectrum for  $E_i=3.7$  eV exhibits a strong Fano-type resonance. In addition, the spectra for  $E_i=2.3$  and 5.0 eV also show remarkable resonance. These results reveal that the resonance takes place in the whole valence-band region from 0 to 6 eV. As for the spectra for  $E_i=6.4, 7.4,$  and 7.9 eV, these spectra are affected by the background of inelastic secondary electrons which stems from

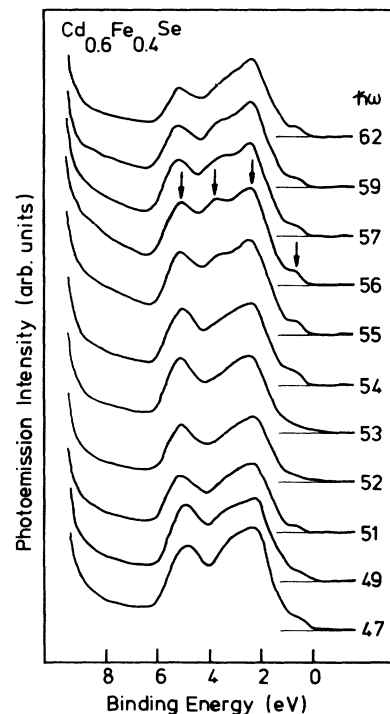


FIG. 2. A series of valence-band spectra of  $\text{Cd}_{0.6}\text{Fe}_{0.4}\text{Se}$  for  $\hbar\omega$  in the Fe  $3p \rightarrow 3d$  excitation region. Four structures at 0.5, 2.3, 3.7, and 5.0 eV below the valence-band maximum are indicated by vertical arrows for the spectrum at  $\hbar\omega=56$  eV. Among these structures, the peak at 3.7 eV exhibits a prominent resonance.

the Fe 3d states, as is clear from Fig. 2. After the correction of the background contribution, however, we still obtain sizable resonance.

In Fig. 4, we compare valence-band spectra of  $\text{Cd}_{0.6}\text{Fe}_{0.4}\text{Se}$  with that of CdSe. According to Fig. 3, the contribution of the Fe 3d emission is at its maximum on resonance ( $\hbar\omega=56$  eV) and at its minimum at the antiresonance ( $\hbar\omega=52$  eV). The latter spectrum of  $\text{Cd}_{0.6}\text{Fe}_{0.4}\text{Se}$  taken at the antiresonance can be regarded as almost due to the emission from the *p* valence bands, without significant contribution of the Fe 3d emission.<sup>8-10</sup> From the comparison of the spectrum of  $\text{Cd}_{0.8}\text{Fe}_{0.4}\text{Se}$  at  $\hbar\omega=52$  eV with that of CdSe, one notices an appearance of the additional *p* DOS in  $\text{Cd}_{0.6}\text{Fe}_{0.4}\text{Se}$  around the energy above the top of the valence band of CdSe (shaded area). An additional DOS is also recognized in the energy region between the two prominent *p* valence bands. An appearance of such new DOS reveals that the band structure of the host CdSe is fairly modified when Fe is added.

Here, we deduce further a measure of the Fe 3d partial DOS in  $\text{Cd}_{0.6}\text{Fe}_{0.4}\text{Se}$ . To this end, we subtract the spectrum measured at the antiresonance ( $\hbar\omega=52$  eV) from that taken just on resonance ( $\hbar\omega=56$  eV), after the normalization of spectral intensities to the monochromator output. The result ("Diff") is shown also in Fig. 4. The Fe 3d partial DOS is superimposed on a background of inelastically scattered electrons. We find structures again at 0.5, 2.3, 3.7, and 5.0 eV below the valence-band maximum

and an appreciable Fe 3d contribution throughout the valence bands from 0 to 6 eV. The full widths at half maximum of the structures at 0.5 and 3.7 eV are estimated to be less than 1 and  $\sim 1$  eV, respectively. Except for these structures at 0.5 and 3.7 eV, one notices that shape of the partial DOS from 0 to 6 eV is very similar to that of the spectrum of CdSe, which is mainly due to the Se 4*p* emission. The spectral density in the energy region deeper than 6 eV is also found.

In the case of  $\text{Cd}_{1-x}\text{Mn}_x\text{Te}$  with a high-spin 3d<sup>5</sup> configuration, the partial DOS has been analyzed in terms of a configuration-interaction (CI) calculation based on a cluster model.<sup>8,9</sup> The photoemission between 0 and 5 eV has been assigned to  $d^5\bar{L}$  final states, which represents final states with a photoproduced *d* hole screened by charge transfer from the Te 5*p*-derived valence bands. Here, the  $\bar{L}$  denotes a ligand hole. Features between 5 and 9 eV, on the contrary, are ascribed to a satellite with  $d^4$  final states without significant *L-d* screening. In spite of the many-body nature of the  $d^5\bar{L}$  final states, we find rather good correspondence between the spectral density from 0 to 5 eV and the one-electron valence-band DOS.<sup>9</sup>

Addition of a 3d $\downarrow$  electron with  $e_g$  symmetry to the  $\text{Mn}^{2+}$  ion with a high-spin 3d<sup>5</sup> ground state realizes an  $\text{Fe}^{2+}$  ion with a high-spin 3d<sup>6</sup> ground state. As concerns the final states of photoemission, the spectral width due to  $d^6\bar{L}$  levels in valence bands would be broader than that for  $d^5\bar{L}$  of  $\text{Cd}_{1-x}\text{Mn}_x\text{Te}$ , since the presence of an additional electron yields further splitting of  $d^5\bar{L}$  levels. Besides, satellite structure with  $d^5$  final states would take

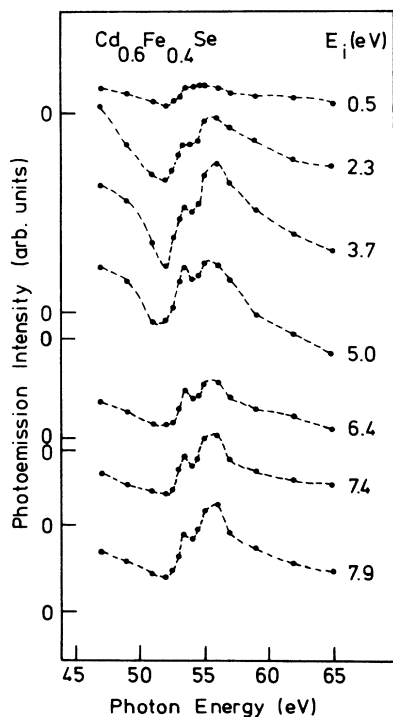


FIG. 3. Plots of the photoemission intensities of selected valence bands as a function of  $\hbar\omega$ . Each valence band is specified by the binding energy ( $E_i$ ) with respect to the valence-band maximum.

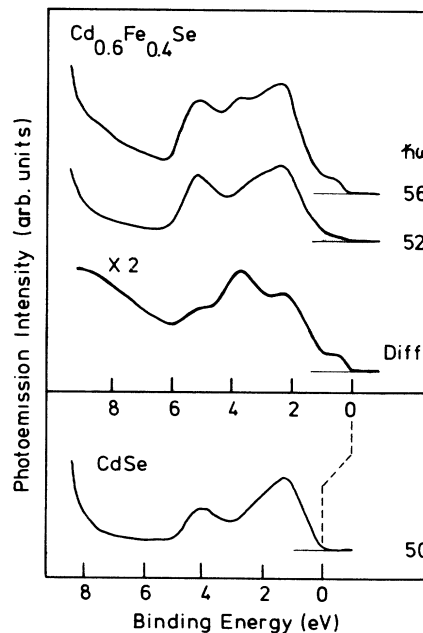


FIG. 4. Valence-band spectra of  $\text{Cd}_{0.6}\text{Fe}_{0.4}\text{Se}$  taken just on resonance ( $\hbar\omega=56$  eV) and at antiresonance ( $\hbar\omega=52$  eV). The difference spectrum "Diff" is a measure of the Fe 3d partial DOS. The spectrum of pure CdSe ( $\hbar\omega=50$  eV) is also shown for comparison.

the form of that satellite due to the  $e_g \downarrow$  electron emission is added to the satellite of  $\text{Cd}_{1-x}\text{Mn}_x\text{Te}$  with  $d^4$  final states. As a result, the characteristic feature of valence bands of  $\text{Cd}_{1-x}\text{Fe}_x\text{Se}$  is expected to be similar to that for  $\text{Cd}_{1-x}\text{Mn}_x\text{Te}$ . Therefore, we can assume that the spectral density between 0 and 6 eV in the Fe 3d partial DOS of  $\text{Cd}_{1-x}\text{Fe}_x\text{Se}$  is due to the  $d^6\bar{L}$  screened final states while that in the deeper binding energy stems from the  $d^5$  poorly screened final states.

We further remember that the resonance in Fig. 3 is due to an interference between the direct excitation process of the Fe 3d electrons and the discrete Fe  $3p \rightarrow 3d$  excitation process followed by a super Coster-Kronig decay. When such a resonance takes place, the enhancement for the  $d^5$  final states is expected to show a Fano resonance peak, whereas that for  $d^6\bar{L}$  states exhibits a resonance dip rather than a peak.<sup>11-13</sup> One can recognize that the spectra for  $E_i > 6$  eV show a clear peak at  $\hbar\omega = 56$  eV, while those for  $E_i = 0-6$  eV represent the pronounced dip around  $\hbar\omega = 52$  eV. These results suggest again that the Fe 3d partial DOS between 0 and 6 eV and that at a deeper binding energy are due to the  $d^6\bar{L}$  and  $d^5$  final states, respectively.

Fe 3d- $\text{Se } 4p$  hybridization allows for sufficient screening of the 3d excitations by  $L$ - $d$  charge transfer in the valence bands. In that sense, the spectral density from 0 to 6 eV could be assumed to be a good approximation of a measure of the valence-band DOS. We interpret here the spectral region corresponding to the  $d^6\bar{L}$  final states on the basis of the one-electron band picture just like in the case of  $\text{Cd}_{1-x}\text{Mn}_x\text{Te}$ .<sup>9,10</sup> An energy diagram in Fig. 5 represents schematically the formation of the Fe 3d bands from atomic levels. The degenerate Fe 3d levels are split into a spin-up ( $3d^5$ ) and a spin-down manifold ( $3d^1$ ) due to the intrashell exchange interaction. In the tetrahedral crystal field, the  $3d \uparrow$  and  $3d \downarrow$  states are further split into  $t_{2g} \uparrow$  ( $3d^3$ ),  $e_g \uparrow$  ( $3d^2$ ),  $t_{2g} \downarrow$  (empty), and  $e_g \downarrow$  ( $3d^1$ ) states, respectively. As a result of different degree of the wave-function overlap, we find that there is no strong Se  $4p$ -Fe  $3d$  ( $p$ - $d$ ) hybridization for the Fe  $e_g \uparrow$  and

$e_g \downarrow$  states. These states with  $e_g$  symmetry remain therefore dispersionless and we can identify them with the narrow peaks in the photoemission spectra. On the other hand, the Fe  $t_{2g} \uparrow$  and  $t_{2g} \downarrow$  states hybridize significantly with the Se  $4p$  states ( $\uparrow$  and  $\downarrow$ ) and add the Fe 3d character to the top 6-eV region of the valence bands. Coupling between the spin-up [spin-down] states produces a bonding  $B(\uparrow)$  [ $B(\downarrow)$ ] and an antibonding  $AB(\uparrow)$  [ $AB(\downarrow)$ ] levels. Accordingly, we assign the peaks at 0.5 and 3.7 eV to  $d$  electron emission mainly from the  $e_g \downarrow$  and  $e_g \uparrow$  bands without appreciable dispersion, respectively. Besides, the  $t_{2g} \uparrow$  and  $t_{2g} \downarrow$  bands are spread rather uniformly over the whole valence-band region between 0 and 6 eV due to the strong  $t_{2g} \uparrow(\downarrow) - p \uparrow(\downarrow)$  hybridization. Such uniform distribution of the  $t_{2g}$  states in the valence bands is strongly suggested from the fact that the shape of the portion assigned to the  $t_{2g} \uparrow$  and  $t_{2g} \downarrow$  states in the Fe 3d partial DOS is very similar to that of the Se  $4p$  DOS of CdSe.<sup>14</sup>

Our results on the Fe 3d states in  $\text{Cd}_{1-x}\text{Fe}_x\text{Se}$  are partly in contrast to the model presented earlier.<sup>6</sup> Kisiel *et al.* proposed, based on their optical-reflectivity data, that the Fe 3d levels hybridized with the Se  $4p$  levels appear at the top region of valence bands, while nonhybridized Fe levels are located below the Se  $4p$  valence bands. In our model, the Fe 3d-derived structure observed at the top region of valence bands is due to the final state of photoemission from the  $e_g \downarrow$  state, which does not hybridize appreciably with the Se  $4p$  states. On the basis of CI theory,<sup>15</sup> this structure is assigned to the  ${}^6A_{1g}({}^6S)$  state of the  $d^5$  final-state multiplet ( $t_{2g} \uparrow^3 e_g \uparrow^2 e_g \downarrow^1 \rightarrow t_{2g} \uparrow^3 e_g \uparrow^2$ ). Both one-electron and CI models yield physically the same conclusion for the assignment of the Fe-derived structure at the top region of valence bands. In addition, the Fe 3d states with  $t_{2g}$  symmetry do not appear only around the top region of valence bands as proposed previously,<sup>6</sup> but are spread uniformly over the whole valence-band region.

#### IV. CONCLUSIONS

The contribution of the Fe 3d states to the valence bands of  $\text{Cd}_{1-x}\text{Fe}_x\text{Se}$  has been studied by means of the concentration dependence of the valence-band photoemission spectra and resonant enhancement of the Fe  $3d$  photoemission cross section near the Fe  $3p \rightarrow 3d$  excitation region. Between these two kinds of experiments, the resonant photoemission measurements have facilitated greatly the identification of the Fe 3d-derived features of the valence-band spectra. The Fe 3d partial DOS obtained from the valence-band spectra taken at the antiresonance and on resonance has exhibited four structures at 0.5-, 2.3-, 3.7-, and 5.0-eV binding energies. The narrow peaks at 0.5 and 3.7 eV in the partial DOS are assigned to the  $e_g \downarrow$  and  $e_g \uparrow$  bands, respectively. The structures at 2.3 and 5.0 eV are mainly derived from the  $t_{2g} \uparrow$  and  $t_{2g} \downarrow$  bands, which are spread over uniformly in the valence-band region between 0 and 6 eV through the strong  $p$ - $d$  hybridization. Comparison of the valence-band spectrum

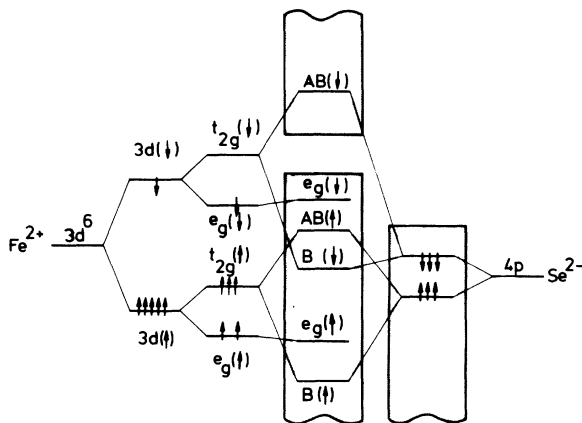


FIG. 5. Schematic energy diagram showing how the Fe 3d-derived DOS is formed from the atomic levels.

of  $\text{Cd}_{0.8}\text{Fe}_{0.4}\text{Se}$  measured at the antiresonance with that of CdSe has revealed the change in the band structure of CdSe due to the presence of Fe atoms. The Fe 3d partial DOS from 0 to 6 eV can be qualitatively understood as due to the final states of *d*-electron emission from the ground states described on the basis of the one-electron band picture.

#### ACKNOWLEDGMENTS

The authors are grateful to Professor A. Fujimori of The University of Tokyo for valuable discussion and critical reading of the manuscript. We thank the staff of SRL-ISSP for the operation of SOR-RING and technical support.

---

<sup>1</sup>N. B. Brandt and V. V. Moschalkov, *Adv. Phys.* **33**, 193 (1984).

<sup>2</sup>*Dilute Magnetic Semiconductors, Semiconductors and Semimetals*, Vol. 25, edited by J. K. Furdyna and J. Kossut (Academic, New York, 1988).

<sup>3</sup>D. Scalbert, J. A. Gaj, A. Mauger, J. Cernogora, and C. B. Guillaume, *Phys. Rev. Lett.* **62**, 2865 (1989).

<sup>4</sup>J. M. Baranowski and J. M. Langer, *Phys. Status Solidi B* **48**, 863 (1971).

<sup>5</sup>A. Mycielski, P. Dzwonkowski, B. Kowalski, B. A. Orlowski, M. Dobrowolska, M. Arciszewska, W. Dobrowolski, and J. M. Baranowski, *J. Phys. C* **19**, 3605 (1986).

<sup>6</sup>A. Kisiel, M. Piacentini, F. Antonangeli, N. Xema, and A. Mycielski, *Solid State Commun.* **70**, 693 (1989).

<sup>7</sup>L. Ley, R. A. Pollak, F. R. McFreely, S. P. Kowalczyk, and D.

A. Shirley, *Phys. Rev. B* **9**, 600 (1974).

<sup>8</sup>L. Ley, M. Taniguchi, J. Ghijsen, and R. L. Johnson, *Phys. Rev. B* **35**, 2839 (1987).

<sup>9</sup>M. Taniguchi, A. Fujimori, M. Fujisawa, T. Mori, I. Souma, and Y. Oka, *Solid State Commun.* **62**, 431 (1987).

<sup>10</sup>M. Taniguchi, A. Fujimori, and S. Suga, *Solid State Commun.* **70**, 191 (1989).

<sup>11</sup>A. Fujimori and A. Minami, *Phys. Rev. B* **30**, 957 (1984).

<sup>12</sup>L. C. Davis, *Phys. Rev. B* **25**, 2921 (1982).

<sup>13</sup>G. Laan, *Solid State Commun.* **42**, 165 (1982).

<sup>14</sup>A. Goldmann, J. Tejada, N. J. Shevchik, and M. Cardona, *Phys. Rev. B* **10**, 4388 (1974).

<sup>15</sup>A. Fujimori, N. Kimizuka, M. Taniguchi, and S. Suga, *Phys. Rev. B* **36**, 6691 (1987).

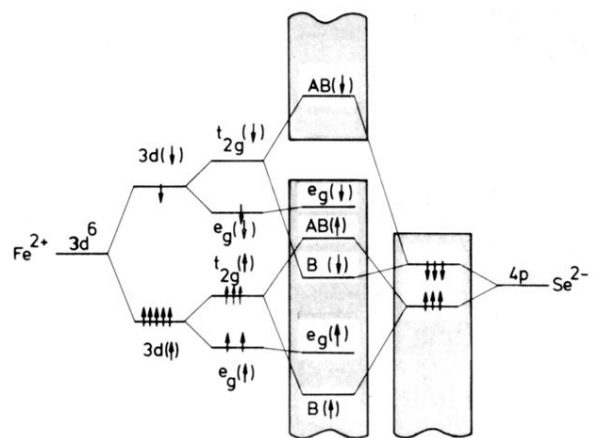


FIG. 5. Schematic energy diagram showing how the Fe 3d-derived DOS is formed from the atomic levels.